Nanobiosensor Design to Detect Cholic Acid Using Multiwalled Carbon Nanotube /TiO_2 Nanoparticle for 3α-Hydroxysteroid Dehydrogenase Immobilization

Jassim, Emad Mohammad; Kashanian, Soheila*[+•]; Nazari, Maryam; Parnianchi, Fatemeh

Faculty of Chemistry, Razi University, Kermanshah, I.R. IRAN

Mahdi, Khudhair M.

Faculty of Education-Chemistry, Thi Qar University, IRAQ

ABSTRACT: *Determination of cholic acid concentration is a useful method to monitor liver diseases. We propose a rapid and simple method for measuring cholic acid. The development of a cholic acid electrochemical biosensor is described that is based on the modification of glassy carbon electrode surface using a mixture of carboxylated multiwalled carbon nanotube and titanium dioxide nanoparticles in chitosan solution and immobilization of 3α-hydroxysteroid dehydrogenase. The modification process of the sensing surface was characterized by Fourier transform infrared spectroscopy, Energy Diverse X-ray Spectrometry, Field Emission Scanning Electron Microscopy, and voltammetry techniques. A good correlation was demonstrated between cholic acid concentration and the peak currents in the presence of nicotinamide adenine dinucleotide. Using a carboxylated multiwalled carbon nanotube and titanium dioxide nanoparticles for electrode modification showed more effective area than an unmodified electrode at optimum pH of 6. Two linear ranges were obtained at 7.1 - 42.7, and 70.9-476.2 nM of cholic acid. Also, the detection limit was 6 nM and the sensitivities of the two ranges were obtained 956.9 and 28.7 μA/μM.*

KEYWORDS: *Biosensor; Cholic acid; 3α-Hydroxysteroid dehydrogenase; Maltiwalled carbon nanotube; Titanium dioxide nanoparticles*

INTRODUCTION

Bile acids are necessary for fat and fat-soluble vitamin absorption by emulsification [1]. They are essential steroidal compounds and definitively metabolized products of cholesterol in the liver; contained primary bile

***** *To whom correspondence should be addressed.*

+ *E-mail: kashanian_s@yahoo.com & s.kashanian@razi.ac.ir*

• *Other Address: Nanobiotechnology Department, Faculty of Innovative Science and Technology, Razi University, P.O. Box 6714414971 Kermanshah, I.R. IRAN*

• *Nano Drug Delivery Research Center, Kermanshah University of Medical Sciences, P.O. Box 6714415153 Kermanshah, I.R. IRAN*

1021-9986/2022/8/2561-2572 12/$/6.02

acids such as Cholic Acid (CA) and chenodeoxycholic acid, and secondary bile acids like lithocholic acid, deoxycholic acid [2]. Furthermore, CA is a significant component of bile acids, and it forms more than 31% of bile acids. CA concentration is related to gallstones, liver cancer, and other diseases [3]. It is generally in the range of 1–5 mM and less than 10 μM in the liver and human serum, respectively [4]. Therefore, developing an approach to sense the level of CA concentration in body fluids is mainly essential.

Several methods have been studied in the literature for CA determination, including high-performance liquid chromatography [5], gas chromatography [6], spectrophotometry [7], fluorimetry [8], solid-phase radioimmunoassay [9], and mass spectrometry [10, 11]. However, these methods need sample pretreatment steps and have disadvantages like costly equipment, time-consuming, and large sample volume, so it is better to develop new benefit methods [4]. Since electrochemical sensors and biosensors have the advantages of ease of procedure, short measuring time, and detection of the biochemical change produced, they are suitable choices for the detection of specific analytes [12, 13]. In recent years, biosensors have been developed to detect CA [14]; however, there is not much research in the field of CA enzymatic-based detection.

Bile acids should be converted to 3-ketosteroids because they do not display electrochemical signals. For this purpose, 3-α-hydroxysteroid dehydrogenase (3α-HSD) can be used in the presence of nicotinamide adenine dinucleotide (NAD^+), which leads to the production of reduced nicotinamide adenine dinucleotide (NADH); therefore, NADH can be oxidized on the electrode surface to produce obvious electrochemical signals. Consequently, the bile acid concentration can be sensed by electrochemical signals [15]. For the construction of biosensors, it is better to immobilize 3α-HSD on the electrode surface. Enzyme immobilization offers advantages such as reusability and prevention of enzyme leakage. Different ways can be applied for enzyme immobilization, including entrapment, physical adsorption, cross-linking, and covalent bonding [16, 17]. The most stable approach for enzyme immobilization is using covalent bonds [18, 19].

Nanomaterials are attractive in developing electrochemical biosensors [20]. Carbon NanoTubes (CNTs) have a high surface area and unique mechanical and electrical properties and are proven to stimulate electron transfer between electrodes and electrochemically active compounds [21]. In addition, to make a high effective surface area, MWCNT-COOH can be used for enzyme immobilization. *Yadav et al*. fabricated an oxalate biosensor based on carboxylated multiwalled carbon nanotube/polyaniline (MWCNT-COOH/PANI) nanocomposite which provides covalent linkage between enzyme and electropolymerized c-MWCNT/PANI composite film using coupling agents N-hydroxy succinimide (NHS) and N-ethyl-N-(3-dimethylaminopropyl) carbodiimide (EDC) [22].

Cerium oxide (CeO_2) [23], zinc oxide (ZnO) [24], zirconium oxide (ZrO_2)[25], and titanium oxide (TiO_2) [26], as nanoporous metal oxide nanoparticles, have been used for the fabrication of enzyme-based biosensors. Amongst them, TiO_2 NPs have enticed much attention owing to their unique properties, such as preservation of biological activities, biocompatibility, and excellent mechanical strength [27]. TiO_2 NPs have been used for analyte detection with acceptable detection limits [28, 29]. Using TiO_2NPs can improve NADH oxidation and analyte detection [30]. *Fan et al.* used Au-TiO_2/graphene nanocomposite for electrochemical sensing of hydrogen peroxide and NADH [30]. However, TiO_2/graphene nanocomposite did not get a clear redox current peak for NADH, but using Au-TiO_2/graphene has shown remarkable redox current peaks for NADH detection compared to Au/graphene. In another work, *Jiang et al.* used TiO_2/ MWCNTs electrodes for hydrogen peroxide detection. Compared with MWCNTs, the TiO_2/MWCNTs electrode presents a fast response, is stable, low-potential, and highly sensitive to the detection of hydrogen peroxide [31]. *Li et al.* used TiO_2-Au nano-clusters onto MWCNTs and reduced graphene hybrid nanocomposites due to facilitating the direct electron transfer and enhancing the catalytic activity of electrochemical sensing [32].

Chitosan (CHIT) is a natural polysaccharide that improves enzyme retaining and has suitable film formation and good adhesion properties [16, 33]. Also, the use of CHIT can prevent the aggregation of CNTs [33]. CHIT can be bound with nanomaterials simply because of amino ($-NH_2$) and hydroxyl (-OH) groups [34]. A glassy carbon electrode (GCE) is a very useful tool for the detection of analytes in electrochemical methods and its modification by nanomaterials and enzymes improves detections. *Mehdizadeh et al.* modified GCE by glucose oxidase (GOD)/chitosan (CHIT)/Graphene Oxide (GO) nanofibers

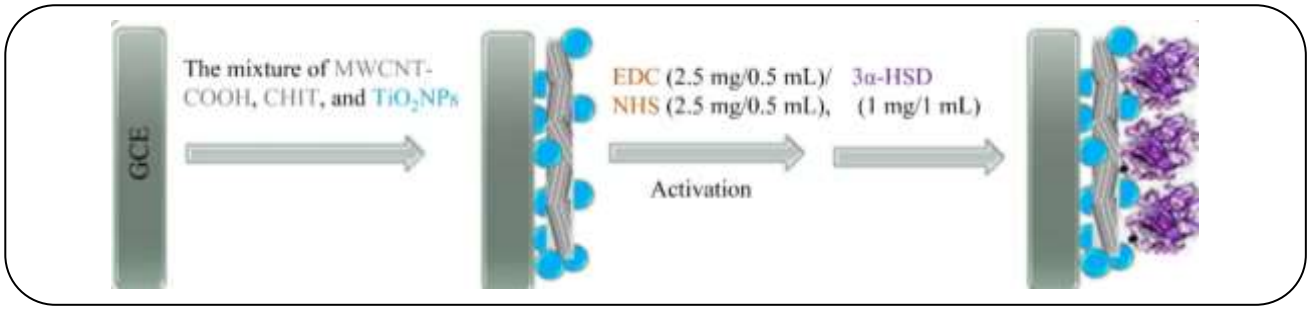

Scheme 1: Schematic representation of conjugation of 3α-HSD to MWCNTs-COOH using EDC and NHS.

and used this modified electrode for glucose detection [35]. In another study, *Rubio-Govea et al.*, modified the GCE surface using MoS_2 nanostructured materials and laccase for dopamine detection [36]. *Haritha et al.* used nanoscale metal cluster-loaded MWCNTs and cholesterol oxidase (COx) for the modification of GCE and cholesterol detection [37].

The aim of this project is to build up a novel electrochemical biosensing electrode for CA detection using covalently immobilized 3α-HSD on GCE modified by the mixture of MWCNT-COOH and TiO_2 NPs in CHIT solution. This study, for the first time, uses the mentioned composition for 3α-HSD immobilization and CA detection.

EXPERIMENTAL SECTION

Reagents and materials

3α-HSD and CA were supplied by Sigma-Aldrich. Also, NHS and EDC were obtained from Sigma-Aldrich. Titanium and MWCNT-COOH were purchased from Merck and US Research Nanomaterials, Inc., respectively. CHIT (deacetylation grade of about 90.28% and average Mw of 100-300 kg/mol) was purchased from MP Biomedicals, LLC (Solon, OH 44139). All other materials were obtained from Merck.

Three electrodes, including GCE (Working electrode), Ag/AgCl (saturate, 3M KCl) (Reference electrode), and Platine wire (Counter electrode) were applied to carry out electrochemical experiments, which were obtained from the Azar electrode. They were connected to the electroanalyzer of SAMA 500. Fourier transform infrared (FTIR) spectrum (Bruker Company) was recorded between the ranges of 400-4000 cm^{-1}. Field emission scanning electron microscopy (FESEM) (Mira3te) and Energy Diverse X-ray Spectrometry (EDS) were used to characterize electrode surfaces.

Synthesis of TiO_2 NPs

The synthesis method of TiO_2 NPs was applied in the literature [38]. Briefly, water, glacial acetic acid, and titanium (IV) isopropoxide were maintained using the molar ratio of 350:10:1. First, a solution was synthesized by adding glacial acetic acid at 0 ◦C to titanium (IV) isopropoxide, and then, under vigorous stirring for 1h, water was added to this solution dropwise. For 30 min, the resultant solution was ultrasonicated; after a further 5 h, it was stirred till producing a clear solution of TiO_2 nanocrystals. After that, it was incubated at 70 ◦C for 12 h, and at 100 ◦C, the obtained gel was dried and crushed into satisfactory powder; then, at 500 ◦C for 5 h, it was calcined to form TiO_2 NPs.

Preparation of MWCNT-COOH and TiO_2 NPs mixture in CHIT solution

The mixture of MWCNT-COOH and TiO_2 NPs was prepared in chitosan solution. For this purpose, CHIT (5 mg) was dispersed in an acetic acid solution (1 mL of 1 % v/v), then it was added to a dispersion of MWCNT-COOH (2 mg) and TiO_2 NPs (2 mg) under ultrasonication for 24 h to get a black mixture. The mixture was stored in the refrigerator at 4 °C.

Immobilization of 3α-HSD onto the modified electrode surface

After polishing GCE with alumina slurries and fine emery paper, it was rinsed with ultrapure water and dried at room temperature. Then 7 µL of the black mixture (1 mg/mL) was dropped on the electrode surface; after drying, 7 µL of EDC (5%) and NHS (5%) were dropped on the electrode surface respectively, as shown in Scheme 1. After drying, the 3α-HSD solution (1 mg/mL; pH 7) was dropped on the electrode surface. The modified electrode surface morphology was characterized by FESEM, EDS,

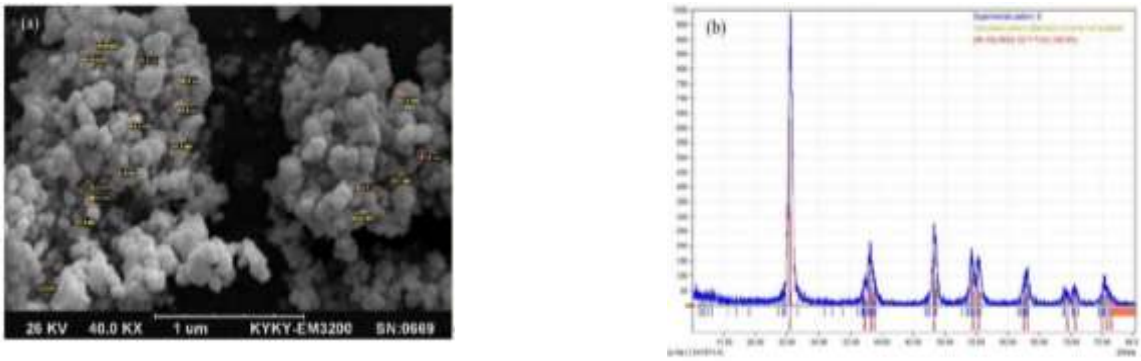

Fig. 1: (a) SEM image of TiO_2 NPs calcined at 500 ◦C. (b) XRD patterns of TiO_2 NPs prepared from Ti(IV) isopropoxide calcined at 500 °C.

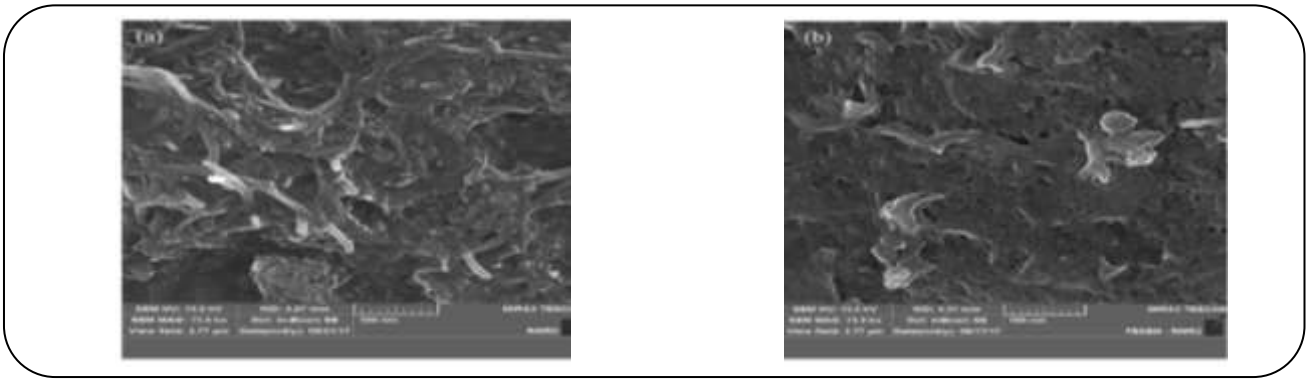

Fig. 2: FESEM images of electrode surfaces modified with (a) TiO_2, MWCNT-COOH, CHIT/GCE, (b) 3α-HSD/TiO_2, nMWCNT- COOH, CHIT/GCE.

and FT-IR. Additionally, cyclic voltammetry (CV) and Differential Pulse Voltammetry (DPV) techniques were employed to study the electrochemical behaviors of modified electrodes. When the biosensor was not used, it was stored in the refrigerator at 4 °C.

RESULTS AND DISCUSSION

Morphological investigation of TiO_2 NPs

Fig. 1 displays the SEM image and XRD spectra of calcined TiO_2 NPs. TiO_2 NPs are spherical and cluster-like structures with a grain size minimum of 50 nm according to the SEM image (Fig. 1a). The patterns of XRD spectra show the calcined TiO_2 NPs structure (Fig. 1b). The diffraction peaks demonstrate that the prepared sample is in anatase structure, and precisely all of the peaks are provided the same as TiO_2 NPs [38]. Hence, SEM image and XRD results are consistent and confirmed TiO_2 NPs synthesis.

Biosensor morphological investigation

Fig. 2 exhibits the FESEM images of TiO_2NPs,MWCNT-COOH,CHIT/GCE, 3α-HSD/TiO_2NPs,MWCNT-COOH,CHIT/GCE. Fig. 2a shows the nanotubes form of MWCNT-COOH and spherical TiO_2NPs,MWCNTs-COOH,CHIT that is a porous structure. Therefore, it is concluded that the MWCNT-COOH and TiO_2 NPs are successfully deposited on the GCE, and the image clearly proves that TiO_2 NPs and MWCNTs-COOH were scattered on the surface of GCE. According to Fig. 2b, the nanotubes form of MWCNT-COOH were changed after immobilizing of 3α-HSD due to the formation of covalent binding between the NH_2 group of 3α-HSD and COOH group of MWCNT, and it confirms the presence of 3α-HSD spots on the modified GCE.

Fig. 3a (curves 1& 2) shows the FTIR spectra of two different electrodes in the range of 400 to 4000 cm^{-1}. According to Fig. 3a, the peaks of 3429 related to the curve

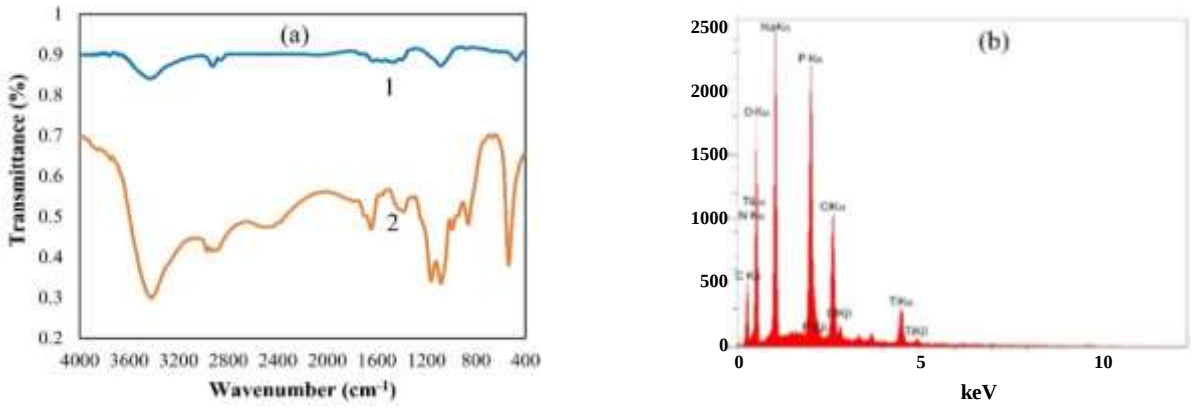

Fig. 3: (a) Infrared absorption spectra of the electrodes; TiO_2, MWCNT-COOH, CHIT/GCE (1), and 3α-HSD/TiO_2, MWCNT-COOH, CHIT/GCE (2). (b) EDS analysis of 3α-HSD/TiO_2, MWCNT, CHIT/GCE.

1 and 342 cm^{-1} related to curve 2 are attributed to O-H (functional group of MWCNT-COOH) and NH_2 (functional group of CHIT). Also, the peaks of 2860 and 2924 are related to asymmetric/symmetric methylene stretching bands of MWCNT-COOH for curve 1. The peaks of 1730 and 1566 cm^{-1} are related to carboxyl functional groups on MWCNT-COOH surface [39]. The peaks of 1631 and 1083 cm^{-1} are attributed to C=O and C-O stretching bands of CHIT (Fig. 3a curve 1) [40, 41]. The peak at 535 cm^{-1} in curve 2 displays the stretching vibration of Ti-O-Ti (the functional group of TiO_2NPs) [42]. According to curve 2 (Fig. 3a), appearing the peak in 1706 cm^{-1} is related to the binding of 3α-HSD to MWCNT-COOH [43].

EDS spectrum of 3α-HSD/TiO_2NPs, MWCNT-COOH, CHIT/GCE showed the presence of C, O, N, Na, P, Cl, and Ti elements on the electrode surface (Fig. 3b).

Electrochemical measurements

The conducting properties of electrodes and the kinetics of redox reactions can be studied under intensive controlled conditions using CV. Electrochemical parameters were considered including the redox peak currents and potentials. E_p^a and i_p^a are considered as anodic peak potential and current, respectively, and E_p^c and i_p^c are considered as cathodic peak potential and cathodic peak current, respectively. It was considered to examine the behavior changes of the modified electrodes; MWCNT-COOH, CHIT/GCE, TiO_2NPs, MWCNT-COOH, CHIT/GCE, and 3α-HSD/TiO_2NPs, MWCNT-COOH, CHIT/GCE.

The electrochemical behavior and the oxidation/ reduction properties of electrodes were investigated by CV in a phosphate buffer (PB) solution. Electrochemical biosensors based on NADH oxidation are of great interest for substrate detection and, hence, NADH electrochemically monitoring is an advantage due to the nonelectroactive nature of substrates. However, NADH electrochemical oxidation to NAD^+ occurred at high overpotentials on the surface of bare electrodes, and using some mediators or NPs can reduce this overpotential [44]. According to Fig. 4a, 3α-HSD/TiO_2NPs, MWCNT-COOH, CHIT/GCE has distinctive anodic peak compared to GCE and other modified electrodes in the presence of NADH and CA; while there is not seen any anodic and cathodic peaks for TiO_2NPs,MWCNT-COOH,CHIT/GCE in the presence or absence of NADH and CA. The data of redox currents and potentials are shown in Table 1. These results show that the 3α-HSD-based biosensor has a significant anodic current to detect cholic acid due to a 2.7-fold increase of anodic current in the presence of NADH compare to the state without NADH; NADH is an electrochemical redox active cofactor for 3α-HSD [45, 46].

pH effect

pH is one of the critical parameters that affect enzymatic reactions. For showing maximal activity, enzymes should be used at optimal pH. The activity of 3α-HSD is generally investigated in the pH range between 5.5 to 10 [47]. Therefore, the 3α-HSD-based biosensor was investigated in PB solution with a more extensive range pH values (4.0 to 11.0) (Fig. 4b). The optimum pH was found to be 6 because it has a higher current in this pH than other pHs for NADH oxidation. In pHs more and less than 6, the current peaks are decreased, maybe due to the enzymatic activity decline [48]. Consequently, pH 6 was used for further determination of CA at the biosensor.

Table 1: Voltammogram data of 3α-HSD/TiO_2,MWCNT-COOH,CHIT/GCE in PB (0.1 M) at pH 6 in the (a) presence and absence (b) of NADH. Scan rate: 0.1 V/s.

Electrode		E_p^a (V)	E_p^c (V)	I_p^a (µA)	I_p^c (µA)	E_p^a - E_p^c (V)
3α-HSD/TiO_2,MWCNT-COOH,CHIT/GCE	Without NADH	0.093	0.015	0.26	-0.18	0.078
3α-HSD/TiO_2,MWCNT-COOH,CHIT/GCE	With NADH	0.36	-	0.7	-	-

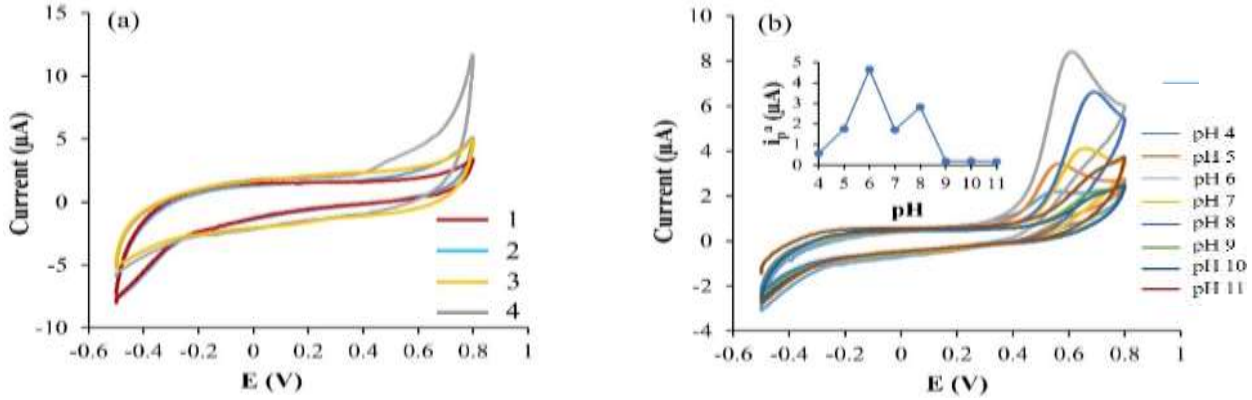

Fig. 4: Cyclic voltammograms of GCE (1), MWCNT-COOH,CHIT/GCE (2), TiO_2,MWCNT-COOH,CHIT/GCE (3), and 3α-HSD/TiO_2,MWCNT-COOH,CHIT/GCE (4) in 0.1 M PB at pH 6 containing NADH (0.006 M) and CA (10 µM); Scan rate: 0.1 V/s (a). The effect of pH on the current responses of NADH oxidation and reduction for 3α-HSD/TiO_2, MWCNT-COOH,CHIT/GCE in 0.1 M PB containing NADH (0.006 M) and CA (10 µM); Scan rate: 0.1 V/s (b).

Scan rate effect

Using CV to study scan rate influence on redox currents and potentials is one of the most effective techniques, which clarifies the redox properties of the substrates. A series of scan rate values (in the range of 0.02-1 V/s) was selected to investigate the scan rate effect on the biosensor response.

Fig. 5a demonstrates the voltammograms of the proposed biosensor in the absence of NADH. By increasing the scan rates, increasing the redox peaks is seen, and found the linear relationship between the scan rate and peak currents with a correlation coefficient of 0.96 for anodic and 0.97 for cathodic currents as shown in Fig. 5b. Adsorption is the main mechanism because of the high correlation coefficient in the relation of currents and scan rate; when the plot of peak currents versus the scan rate is more linear than the plot of peak currents versus the square of scan rate confirms the adsorption mechanism [49, 50]. Furthermore, increasing the scan rates results in shifting the anodic and cathodic peak potentials to the positive and negative directions, respectively (Fig. 5c); this behavior occurs when the mechanism of electron transferring on the electrode surface is quasi-reversible [41].

The voltammograms of the proposed biosensor in the presence of NADH are given in Fig. 6a. With increasing the scan rates, the anodic peak potential slightly shifted to the positive potential direction. There is no cathodic peak, but the oxidation peak currents increased with increasing the scan rates, and a linear relationship is found between them and the scan rates, with a correlation coefficient of 0.97 (Fig. 6b); this obtained line results in the adsorption behavior [51]. When the current has a linear relationship with increasing scan rate, the mechanism is adsorption and the molecule is adsorbed on the electrode surface while the linear relationship between the current and the square of the scan rate shows a diffusion mechanism [52, 53].

Calculation of the effective surface area

The effective surface area (A) of modified electrodes was estimated by cyclic voltammograms using $K_3[Fe(CN)_6]$ (5 mM) as a probe at various scan rates. Peak current (I_p) changes linearly versus the square of scan rate according to Randles–Sevick equation and the slope, and then the value of A can be obtained. The subsequent Randles–Sevick formula can be applied for a reversible process [53-55]:

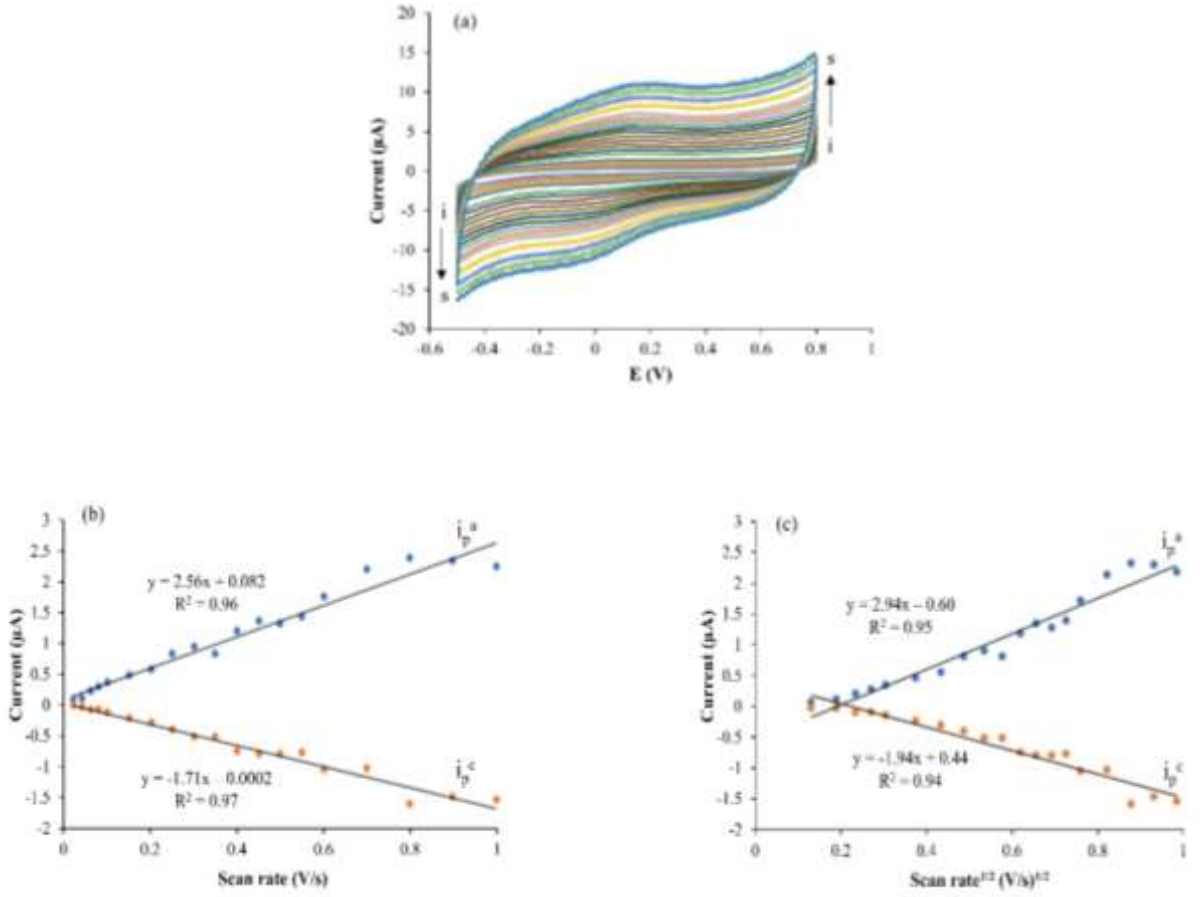

Fig. 5: Cyclic voltammograms of 3α-HSD/TiO₂,MWCNT-COOH,CHIT/GCE in 0.1 M PB pH 6. Scan rates; 0.02, 0.04, 0.06, 0.08, 0.12, 0.14, 0.16, 0.18, 0.2, 0.25, 0.3, 0.35, 0.4, 0.45, 0.5, 0.6, 0.7, 0.8, 0.9 to 1 V/s, respectively (a). The relationship between redox peak currents with the scan rate for 3α-HSD/TiO₂,MWCNT-COOH,CHIT/GCE (b). The relationship between redox peak currents with the square root of scan rate for 3α-HSD/TiO₂,MWCNT-COOH,CHIT/GCE (c).

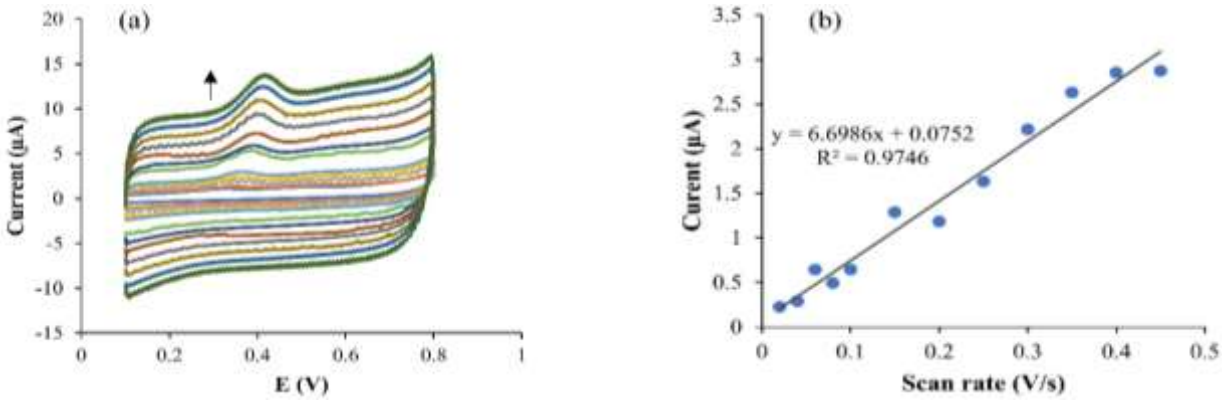

Fig. 6: Cyclic voltammograms of 3α-HSD/TiO₂,MWCNT-COOH,CHIT/GCE in 0.1 M PB pH 6 in the presence of NADH (0.006 M) and CA (10 μM). Scan rates; 0.02, 0.04, 0.06, 0.08, 0.12, 0.14, 0.16, 0.18, 0.2, 0.25, 0.3, 0.35, 0.4, to 0.45 V/s, respectively (a). The relationship between anodic peak currents with the scan rate for 3α-HSD/TiO₂,MWCNT-COOH,CHIT/GCE (b).

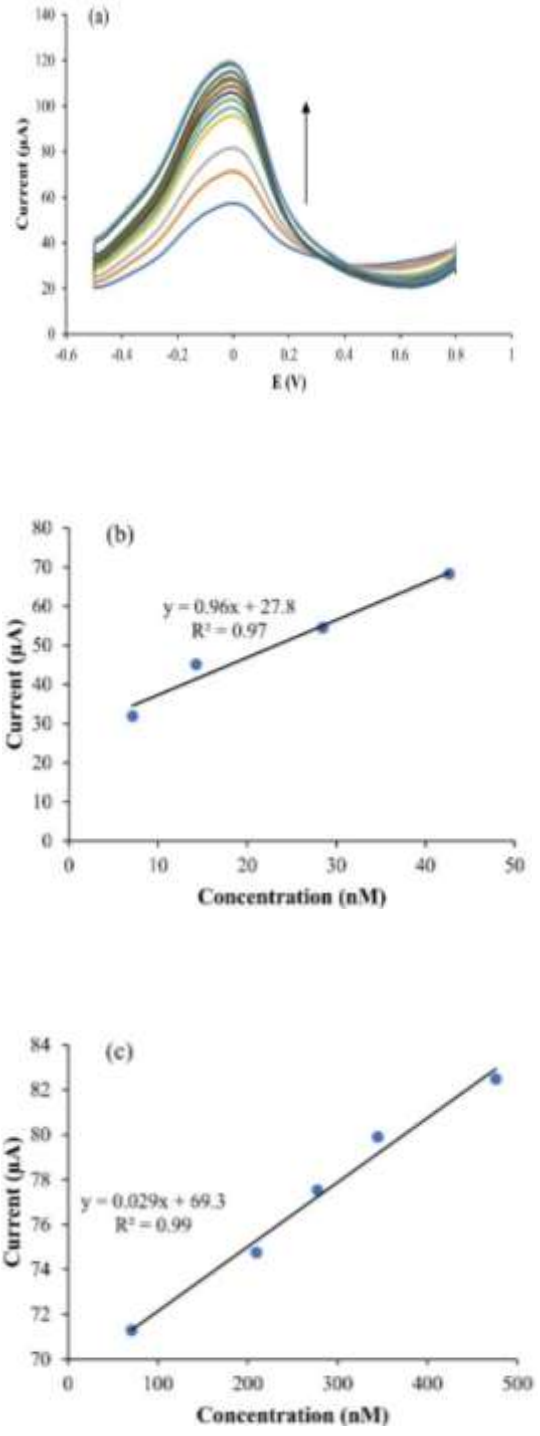

Fig. 7: Illustration of the DPV of 3α-HSD/TiO_2, MWCNT-COOH,CHIT/GCE for different CA concentrations in PB solution pH 6 containing NADH (0.006 M). Electrode area: 1.5 cm^2; scan rate: 0.1 V/s (a). CA calibration curve for 3α-HSD/TiO_2,MWCNT-COOH,CHIT/GCE in the concentration range of 7.1-42.7 nM (b) and 70.9-476.2 nM (c).

$$I_p = \left(2.69\times10^5\right) n^{3/2} A D^{1/2} \upsilon^{1/2} C^0 \quad (1)$$

For 5 mM $K_3[Fe(CN)_6]$, n = 1, D = 7.6 × 10^{-6} cm^2/s, then the effective A of modified electrodes were estimated. The slope was 37.9, 189.8, 237.4 μA/$(V/s)^{0.5}$ for GCE, MWCNT-COOH/GCE, and TiO_2, MWCNT-COOH/GCE, respectively. Then, the A of the electrode was calculated to be 1.02, 5.12, and 6.40 mm^2 for GCE, MWCNT-COOH/GCE, and TiO_2, MWCNT-COOH/GCE, respectively. The effective A of the TiO_2, MWCNT-COOH/GCE is 6.27 times larger than the bare electrode and it confirmed that the bare GCE has been efficiently modified.

Calibration curve

According to Fig. 7, the calibration curve and DPV were demonstrated in various concentrations for CA detection. The PB solution (0.1 M, pH 6) containing NADH (0.006 M) was used, and the relationship between the CA concentrations and the biosensor anodic current was followed by DPV technique (Fig. 7a). Limit of detection (LOD) was calculated by considering the relation between standard deviation (σ) and the slope (m) of the calibration curve (3σ/m); it was obtained 6 nM. Also, two concentration ranges of 7.1-42.7 and 70.9-476.2 nM were obtained, and the sensitivities (the slope of calibration curves) of these two ranges were 956.9 and 28.7 μA/μM, respectively (Fig. 7 b,c).

The behavior of diverse approaches for CA detection is compared in Table 2. LOD of the presented biosensor is the lowest compared to the LOD of the other techniques for CA recognition.

CONCLUSIONS

The immobilization of 3α-HSD on TiO_2,MWCNT-COOH,chit/GCE was studied via a covalent bond method. This procedure is regarded as a simple and highly versatile method for the incorporation of components into film structures. By exploiting the chemical properties of CA and the multifunctional catalytic properties of 3α-HSD, as well as the electrochemical properties of MWCNT-COOH and TiO_2 NPs, we have successfully developed a novel electrochemical method for a higher sensitive determination of CA. The proposed biosensor combines the properties of MWCNT-COOH to reduce the oxidation potential with the attractive electrocatalytic properties

Table 2: Comparable methods for determination of CA.

Method	Enzyme	Optimum pH	Analyte	Linear range	LOD	Sensitivity	Ref
Optical, Free enzyme	3α-HSD	9	Total bile acid	0.5-180 µM	0.22 µM	-	[57]
MIP based QCM nanosensor	-	-	CA	0.01-1000 µM	0.0065 µM	14.87 µA/µM	[58]
HPLC	-	-	CA	-	4.27 µM	-	[59]
Fluorescent sensors (β- cyclodextrin-modified carbon dot nanoprobes)	-	7.4	CA	0-650 µM	25 nM	-	[60]
LSPR (aptamer–Au NPs biosensor)	-	7.6	CA	-	1 µM	-	[61]
Enzyme-based electrochemical biosensor	3α-HSD	6	CA	7.1 - 42.7 nM 70.9-476.2 nM	6 nM	956.9 and 28.7 µA/µM	This work

Quartz crystal microbalance (QCM); Localized surface plasmon resonance (LSPR)

of TiO_2 NPs promote a faster electron transfer rate; they have significant effects which cause to increase the electrode A. Furthermore, the obtained effective A for the electrode modified with these nanomaterials was 6.27 times more than that of the bare electrode. The biosensor structure can provide a large effective A for excellent adsorption and diffusion of NADH and CA to improve the response properties of the electrochemical enzyme biosensor. The resulting data of the proposed biosensor demonstrates a low LOD, high sensitivity, and wide linear range.

Received : Jul. 23, 2021 ; Accepted : Oct. 11, 2021

REFERENCES

[1] Kim H.J., Jang C.-H., Liquid Crystal-Based Capillary Sensory Platform for the Detection of Bile Acids, *Chem. Phys. Lipids.*, **204**: 10-14 (2017).

[2] Rössger K., Charpin-El-Hamri G., Fussenegger M., Bile Acid-Controlled Transgene Expression in Mammalian Cells and Mice, *Metab. Eng.*, **21**: 81-90 (2014).

[3] He S., Liang W., Tanner C., Cheng K.-L., Fang J., Wu S.-T., Liquid Crystal Based Sensors for the Detection of Cholic Acid, *Anal. Methods*, **5**: 4126-4130 (2013).

[4] Niu X., Luo D., Chen R., Wang F., Sun X., Dai H., Optical Biosensor Based on Liquid Crystal Droplets For Detection of Cholic Acid, *Opt. Commun.*, **381**: 286-291 (2016).

[5] Okuda H., Obata H., Nakanishi T., Hisamitsu T., Matsubara K., Watanabe H., Quantification of Individual Serum Bile Acids in Patients with Liver Diseases Using High-Performance Liquid Chromatography, *Hepato-Gastroenterology.*, **31**: 168-171 (1984).

[6] Ghaffarzadegan T., Nyman M., Jönsson J.Å., Sandahl M., Determination of Bile Acids by Hollow Fibre Liquid-Phase Microextraction Coupled with Gas Chromatography, *J. Chromatogr. B Biomed. Appl.*, **944**: 69-74 (2014).

[7] Mashige F., Tanaka N., Maki A., Kamei S., Yamanaka M., Direct Spectrophotometry of Total Bile Acids in Serum, *Clin. Chem.*, **27**: 1352-1356 (1981).

[8] Xu Z., Deng P., Tang S., Li J., Fluorescent Molecularly Imprinted Polymers Based on 1, 8-Naphthalimide Derivatives for Efficiently Recognition of Cholic Acid, *Mater. Sci. Eng. C.*, **58**: 558-567 (2016).

[9] Van den Berg J., Van Blankenstein M., Bosman-Jacobs E.P., Frenkel M., Hörchner P., Oost-Harwig O.I., Wilson J., Solid Phase Radioimmunoassay for Determination of Conjugated Cholic Acid in Serum, *Clin. Chim. Acta*, **73**: 277-283 (1976).

[10] Sarafian M.H., Lewis M.R., Pechlivanis A., Ralphs S., McPhail M.J., Patel V.C., Dumas M.-E., Holmes E., Nicholson J.K., Bile Acid Profiling and Quantification in Biofluids Using Ultra-Performance Liquid Chromatography Tandem Mass Spectrometry, *Clin. Chim. Acta*, **87**: 9662-9670 (2015).

[11] Birk J.J., Dippold M., Wiesenberg G.L., Glaser B., Combined Quantification Of Faecal Sterols, Stanols, Stanones and Bile Acids in Soils and Terrestrial Sediments by Gas Chromatography–Mass Spectrometry, *J. Chromatogr. A*, **1242**: 1-10 (2012).

[12] Rotariu L., Lagarde F., Jaffrezic-Renault N., Bala C., Electrochemical Biosensors for Fast Detection of Food Contaminants–Trends and Perspective, *Trends Analyt. Chem.*, **79**: 80-87 (2016).

[13] Nazari M., Kashanian S., Moradipour P., Maleki N., A Novel Fabrication of Sensor Using ZnO-Al_2O_3 Ceramic Nanofibers to Simultaneously Detect Catechol and Hydroquinone, *J. Electroanal. Chem.*, **812**: 122-131 (2018).

[14] Klouda J., Nesměrák K., Kočovský P., Barek J., Schwarzová-Pecková K., A Novel Voltammetric Approach to the Detection of Primary Bile Acids in Serum Samples, *Bioelectrochemistry*, 107539 (2020).

[15] Lawrance D., Williamson C., Boutelle M., Cass A., Development of a Disposable Bile Acid Biosensor for Use in the Management of Cholestasis, *Anal. Methods.*, **7**: 3714-3719 (2015).

[16] Krajewska B., Application of Chitin-And Chitosan-Based Materials for Enzyme Immobilizations: A Review, *Enzyme Microb. Technol.*, **35**: 126-139 (2004).

[17] Wang D., Jiang W., Preparation of Chitosan-Based Nanoparticles for Enzyme Immobilization, *Int. J. Biol. Macromol.*, **126**: 1125-1132 (2019).

[18] Brena B., González-Pombo P., Batista-Viera F., Immobilization of Enzymes: A Literature Survey, Immobilization of Enzymes and Cells, Springer; p. 15-31 (2013).

[19] Wu J.C.Y., Hutchings C.H., Lindsay M.J., Werner C.J., Bundy B.C., Enhanced Enzyme Stability Through Site-Directed Covalent Immobilization, *J. Biotechnol.*, **193**: 83-90 (2015).

[20] Ji J., Zhou Z., Zhao X., Sun J., Sun X., Electrochemical Sensor Based on Molecularly Imprinted Film at Au Nanoparticles-Carbon Nanotubes Modified Electrode For Determination of Cholesterol, *Biosens Bioelectron.*, **66**: 590-595 (2015).

[21] Kaçar C., Erden P.E., Kılıç E., Amperometric l-lysine Biosensor Based on Carboxylated Multiwalled Carbon Nanotubes-SnO_2 Nanoparticles-Graphene Composite, *Appl. Surf. Sci.*, **419**: 916-923 (2017).

[22] Yadav S., Devi R., Kumari S., Yadav S., Pundir C., An Amperometric Oxalate Biosensor Based on Sorghum Oxalate Oxidase Bound Carboxylated Multiwalled Carbon Nanotubes–Polyaniline Composite Film, *J. Biotechnol.*, **151**: 212-217 (2011).

[23] Benjamin S.R., Vilela R.S., Camargo H., Guedes M., Fernandes K.F., Colmati F., Enzymatic Electrochemical Biosensor Based on Multiwall Carbon Nanotubes and Cerium Dioxide Nanoparticles for Rutin Detection, *Int. J. Electrochem. Sci.*, **13**: 563-586 (2018).

[24] Migliorini F.L., Sanfelice R.C., Mercante L.A., Andre R.S., Mattoso L.H., Correa D.S., Urea Impedimetric Biosensing Using Electrospun Nanofibers Modified with Zinc Oxide Nanoparticles, *Appl. Surf. Sci.*, **443**: 18-23 (2018).

[25] Mogha N.K., Sahu V., Sharma M., Sharma R.K., Masram D.T., Biocompatible ZrO_2-Reduced Graphene Oxide Immobilized AChE Biosensor for Chlorpyrifos Detection, *Mater. Des.*, **111**: 312-320 (2016).

[26] Romero-Arcos M., Garnica-Romo M., Martinez-Flores H., Vázquez-Marrufo G., Ramírez-Bon R., González-Hernández J., Barbosa-Cánovas G., Enzyme Immobilization by Amperometric Biosensors with TiO_2 Nanoparticles Used to Detect Phenol Compounds, *Food Eng. Rev.*, **8**: 235-250 (2016).

[27] Parnianchi F., Nazari M., Maleki J., Mohebi M., Combination of Graphene and Graphene Oxide with Metal and Metal Oxide Nanoparticles in Fabrication of Electrochemical Enzymatic Biosensors, *Int. Nano Lett.*, **8**: 229-239 (2018).

[28] Syal A., Sud D., Development of Highly Selective Novel Fluorescence Quenching Probe Based on Bi2S3-TiO2 Nanoparticles for Sensing the Fe (III), *Sens. Actuators B Chem.*, **266**: 1-8 (2018).

[29] Azin Z., Pourghobadi Z., Electrochemical Sensor Based on Nanocomposite of Multi-Walled Carbon Nano-Tubes (MWCNTs)/TiO_2/Carbon Ionic Liquid Electrode Analysis of Acetaminophen in Pharmaceutical Formulations, *Iran. J. Chem. Chem. Eng. (IJCCE)*, **40**: 1030-1041 (2021).

[30] Fan Y., Yang X., Yang C., Liu J., Au- TiO_2/Graphene Nanocomposite Film for Electrochemical Sensing of Hydrogen Peroxide and NADH, *Electroanalysis*, **24**: 1334-1339 (2012).

[31] Jiang L.C., Zhang W.D., Electrodeposition of TiO_2 Nanoparticles on Multiwalled Carbon Nanotube Arrays for Hydrogen Peroxide Sensing, *Electroanalysis*, **21**: 988-993 (2009).

[32] Li J., Wang X., Duan H., Wang Y., Luo C., Ultra-Sensitive Determination of Epinephrine Based on TiO_2-Au Nanoclusters Supported on Reduced Graphene Oxide and Carbon Nanotube Hybrid Nanocomposites, *Mater. Sci. Eng., C*, **64**: 391-398 (2016).

[33] Salimi A., Pourbahram B., Mansouri-Majd S., Hallaj R., Manganese Oxide Nanoflakes/Multi-Walled Carbon Nanotubes/Chitosan Nanocomposite Modified Glassy Carbon Electrode as a Novel Electrochemical Sensor for Chromium (III) Detection, *Electrochim. Acta*, **156**: 207-215 (2015).

[34] Rao H., Liu Y., Zhong J., Zhang Z., Zhao X., Liu X., Jiang Y., Zou P., Wang X., Wang Y., Gold Nanoparticle/Chitosan@ N, S Co-doped Multiwalled Carbon Nanotubes Sensor: fabrication, Characterization, and Electrochemical Detection of Catechol and Nitrite, *ACS Sustain. Chem. Eng.*, **5**: 10926-10939 (2017).

[35] Mehdizadeh B., Maleknia L., Amirabadi A., Shabani M., Glucose Sensing by a Glassy Carbon Electrode Modified with Glucose Oxidase/Chitosan/Graphene Oxide Nanofibers, *Diam. Relat. Mater.*, **109**: 108073 (2020).

[36] Rubio-Govea R., Hickey D.P., Garcia-Morales R., Rodriguez-Delgado M., Dominguez-Rovira M.A., Minteer S.D., Ornelas-Soto N., Garcia-Garcia A., MoS_2 Nanostructured Materials for Electrode Modification in the Development of a Laccase Based Amperometric Biosensor for Non-Invasive Dopamine Detection, *Microchem. J.*, **155**: 104792 (2020).

[37] Haritha V., Kumar S.S., Rakhi R., Amperometric Cholesterol Biosensor Based on Cholesterol Oxidase and Pt-Au/MWNTs Modified Glassy Carbon Electrode, *Mater. Today: Proc.*, (2021).

[38] Venkatachalam N., Palanichamy M., Murugesan V., Sol–Gel Preparation and Characterization of Nanosize TiO_2: Its Photocatalytic Performance, *Mater. Chem. Phys.*, **104**: 454-459 (2007).

[39] do Amaral Montanheiro T.L., Cristóvan F.H., Machado J.P.B., Tada D.B., Durán N., Lemes A.P., Effect of MWCNT Functionalization on Thermal and Electrical Properties of PHBV/MWCNT Nanocomposites, *J. Mater. Res.*, **30** :55-65 (2015).

[40] Mallakpour S., Madani M., Synthesis, Structural Characterization, and Tensile Properties of Fructose Functionalized Multi-Walled Carbon Nanotubes/ Chitosan Nanocomposite Films, *J. Plast. Film Sheeting*, **32**: 56-73 (2016).

[41] Pavia D., Lampman G., Kriz G., Vyvyan J., "Introduction to Spectroscopy Cengage Learning", Ainara López Maestresalas (2014).

[42] Zhang H., Wang X., Li N., Xia J., Meng Q., Ding J., Lu J., Synthesis and Characterization of TiO_2 /Graphene Oxide Nanocomposites for Photoreduction of Heavy Metal Ions in Reverse Osmosis Concentrate, *RSC Adv.*, **8**: 34241-34251 (2018).

[43] Batra B., Pundir C., Construction and Application of β-(3-N-oxalyl-l-2, 3-diaminopropanoic acid) Biosensor Based on Carboxylated Multiwalled Carbon Nanotubes/Gold Nanoparticles/Chitosan/Au Electrode, *RSC Adv.*, **4**: 42723-42731 (2014).

[44] Teymourian H., Salimi A., Hallaj R., Low Potential Detection of NADH Based on Fe_3O_4 Nanoparticles/ Multiwalled Carbon Nanotubes Composite: Fabrication of Integrated Dehydrogenase-Based Lactate Biosensor, *Biosens. Bioelectron.*, **33**: 60-68 (2012).

[45] Teodorczyk M., Purdyt W.C., An Amperometric Enzyme Electrode for the Determination of 3α-Hydroxysteroids, *Talanta*, **37**: 795-800 (1990).

[46] Mundaca R., Moreno-Guzmán M., Eguílaz M., Yáñez-Sedeño P., Pingarrón J., Enzyme Biosensor for Androsterone Based on 3α-Hydroxysteroid Dehydrogenase Immobilized onto a Carbon Nanotubes/Ionic Liquid/NAD+ Composite Electrode, *Talanta*, **99**: 697-702 (2012).

[47] Jez J.M., Penning T.M., Engineering Steroid 5β-Reductase Activity into Rat Liver 3α-Hydroxysteroid Dehydrogenase, *Biochemistry*, **37**: 9695-9703 (1998).

[48] Zhang M., Yuan R., Chai Y., Li W., Zhong H., Wang C., Glucose biosensor Based on Titanium Dioxide-Multiwall Carbon Nanotubes-Chitosan Composite and Functionalized Gold Nanoparticles, *Bioprocess Biosyst. Eng.*, **34**: 1143-1150 (2011).

[49] Pang Y., Zhang Y., Sun X., Ding H., Ma T., Shen X., Synergistical Accumulation for Electrochemical Sensing of 1-Hydroxypyrene on Electroreduced Graphene Oxide Electrode, *Talanta*, **192**: 387-394 (2019).

[50] Velusamy V., Palanisamy S., Chen S.-W., Balu S., Yang T.C., Banks C.E., Novel Electrochemical Synthesis of Cellulose Microfiber Entrapped Reduced Graphene Oxide: A Sensitive Electrochemical Assay for Detection of Fenitrothion Organophosphorus Pesticide, *Talanta*, **192**: 471-477 (2019)

[51] Tavakolyan Pour F., Waqifhusain S., Rastegar H., Saber Tehrani M., Abroomand Azar P., Electrochemical Oxidation of Flavonoids and Interaction with DNA on the Surface of Supramolecular Ionic Liquid Grafted on Graphene Modified Glassy Carbon Electrode, *Iran. J. Chem. Chem. Eng. (IJCCE)*, **37(3)**: 117-125 (2018).

[52] Guan Q., Guo H., Xue R., Wang M., Zhao X., Fan T., Yang W., Xu M., Yang W., Electrochemical Sensor Based on Covalent Organic Frameworks/MWCNT-NH2/AuNPs for Simultaneous Detection of Dopamine and Uric Acid, *J. Electroanal. Chem.*, **880**: 114932 (2020)..

[53] Baniasadi M., Maaref H., Dorzadeh A., Mohammad Alizadeh P., A Sensitive SiO_2@Fe_3O_4/GO Nanocomposite Modified Ionic Liquid Carbon Paste Electrode for the Determination of Cabergoline, *Iran. J. Chem. Chem. Eng. (IJCCE)*, **39(4)**: 11-22 (2020).

[54] Ngamchuea K., Eloul S., Tschulik K., Compton R.G., Planar Diffusion to Macro Disc Electrodes—What Electrode Size is Required for the Cottrell and Randles-Sevcik Equations to Apply Quantitatively?, *J. Solid State Electrochem.*, **18**: 3251-3257 (2014).

[55] Tamleh Z., Rafipour R., Kashanian S., Protein-Based Nanobiosensor for Electrochemical Determination of Hydrogen Peroxide, *Russ. J. Electrochem.*, **55**: 962-969 (2019).

[56] Zhang G.-H., Cong A.-R., Xu G.-B., Li C.-B., Yang R.-F., Xia T.-A., An Enzymatic Cycling Method for the Determination of Serum Total Bile Acids with Recombinant 3α-Hydroxysteroid Dehydrogenase, *Biochem. Biophys. Res. Commun.*, **326**: 87-92 (2004).

[57] Gültekin A., Karanfil G., Sönmezoğlu S., Say R., Development of a Highly Sensitive MIP Based-QCM Nanosensor For Selective Determination Of Cholic Acid Level in Body Fluids, *Mater. Sci. Eng. C*, **42**: 436-442 (2014).

[58] Ran X., Liang Q., Luo G., Liu Q., Pan Y., Wang B., Pang C., Simultaneous Determination of Geniposide, Baicalin, Cholic Acid and Hyodeoxycholic Acid in Rat Serum for the Pharmacokinetic Investigations by High Performance Liquid Chromatography–Tandem Mass Spectrometry, *J. Chromatogr. B Biomed. Appl.*, **842**: 22-27 (2006).

[59] Lu X., Fan Z., Determination of Cholic Acid in Body Fluids by β‑Cyclodextrin-Modified N-Doped Carbon dot Fluorescent Probes, *Spectrochim. Acta A Mol. Biomol. Spectrosc.*, **216**: 342-348 (2019).

[60] Zhu Q., Li T., Ma Y., Wang Z., Huang J., Liu R., Gu Y., Colorimetric Detection of Cholic Acid Based on an Aptamer Adsorbed Gold Nanoprobe, *RSC Adv*, **7**: 19250-19256 (2017).